



Eco-Friendly Method For Removal Of Some Heavy Metals From Water By Persimmon Leaves Ash And Its Nano Adsorbent: Analytical And Physical Study

Khaled Elgendy*¹, Mounir Zaky¹, Atef Amer¹ and Abd Elnasser Mohammed¹

¹Chemistry Department, Faculty of Science, Zagazig University, Egypt.



Abstract

This study aimed to investigate some heavy metal removal using waste biomass adsorbent persimmon leaves in an aqueous solution. Persimmon leaves, which are biomaterials, have many hydroxyl groups and are highly suitable for removing heavy metals. Therefore, in this study, we investigated the possibility of removing Al, Fe, Pb, and Cd in an aqueous solution using dried persimmon leaves (DPL). Some factors which affected the removal were studied, such as the effect of drying temperature, the quantity of adsorbent, pH, the effect of initial metal ions concentration, the effect of contact time, impact of foreign ion interference, while the best drying temperature was (150, 150, 150, 150 °C) for Al, Fe, Pb, Cd respectively. Furthermore, the best quantity of adsorbent was (1, 0.25, 0.5, 0.5 g) for Al, Fe, Pb, and Cd, respectively. The suitable initial metal ions concentration was 2 mg/L for Al, Fe, Pb, and Cd, respectively. The order of removal efficiency was found to be Fe > Pb > Cd > Al. In another method, some of the DPL was converted to nano powder which was used to investigate the removal of Pb and Cd from aqueous solutions. The nano DPL is more active than the normal DPL. Normal DPL was applied to two samples first one was a sewage water sample, and the other sample was groundwater. The pseudo-second-order model was better suited for the heavy metal adsorption experiments using DPL than the pseudo-first-order model. The adsorption of Al, Fe, Pb, and Cd by DPL was more suitable with the Freundlich isothermal adsorption. It showed an ion exchange reaction in the uneven adsorption surface, indicating that the heavy metal adsorption on DPL was easy. The affinity of heavy metal adsorption to DPL was excellent. This experiment, in which heavy metals are removed using the waste biomass of persimmon leaves, is an eco-friendly bio-adsorbent method because it can remove heavy metals without using chemicals while utilizing waste recycling.

Keywords: Persimmon leaves, adsorption, agricultural waste, nano adsorbent, Heavy metals

1. Introduction

Environmental pollution has become a critical ecological problem. Heavy metals are discharged into the aquatic environment from natural processes like weathering of rocks and volcanic activity, besides industrial processes such as electroplating metallurgy, metal finishing, chemical industrialization, and mining, which causes an increase in heavy metals concentration in the water [1]. Exposure to heavy metals at trace levels is a risk for humans [2]. Hazardous health effects of heavy metals include organ damage, cancer, inhibited growth and development, damage to the nervous system, and death. [3]. Many technologies have been used to

remove heavy metals from the water, like precipitation, adsorption, membrane filtration, and ion exchange [4]. Furthermore, adsorption has been proven efficient and economical for heavy metals removal of organic pollutants and dyes from contaminated waters [5]. The adsorption process features flexibility in operation and design and produces well-treated effluent. Furthermore, adsorbents can be desorbed using a suitable desorption process because adsorption may sometimes be reversible [6]. Several adsorbents, like activated carbon, graphene, and silica, can be used in water purification [7]. The Diospyros kaki (Persimmon) belongs to the Ebenaceae family, with more than 350 species [8]. Currently, China is regarded as the biggest producer of Persimmon in the world, then South

*Corresponding author e-mail: elgendykh64@hotmail.com (Khaled Elgendy);

Received date 21 December 2022; revised date 08 May 2023; accepted date 25 May 2023

DOI: 10.21608/EJCHEM.2023.180192.7367

©2023 National Information and Documentation Center (NIDOC)

Korea and Japan. Ninety-four percent of the world's persimmon production is produced in these three nations. [9]. Persimmon leaves are a natural adsorbent that can be found on farms anywhere as by-products. In addition, persimmon leaves have a lot of polyphenol compounds and tannins, both of which chelate metal ions. [10]. Tannin is a protective agent for plant tissue in plants, but it can also interact with harmful elements like heavy metals [11;12]. Polyphenols are abundant in persimmon fruit [13]; polyphenols refer to a broad class of compounds with multiple phenolic hydroxyl groups linked to one or more benzene ring systems. [14]. persimmon leaves contain the following compounds: 4,4'-dihydroxy- α -truxillic acid, kakispyrone, tatarine-C, quercetin, myricetin, rutin, annulatin, hyperin, trifolin, astragaline, isoquercetin, Kaempferol, and kaki saponin [15].

• **Chemical analysis of Persimmon leaves[16]**

Table (1): Chemical composition of persimmon leaves

Component	%	Component	%
Moisture (%)	8.9	Iron (mg/kg)	374.3
Ash (%)	8.1	Calcium (%)	1.0
Fat (%)	3.84	Phosphorous (%)	0.13
Protein (%)	14.35	Tannins (%)	2.685
Carbohydrates (%)	64.81	Lignin (%)	7.72
Sodium (mg/kg)	341.1	Cellulose (%)	12.84
Potassium(mg/kg)	1352	Hemicellulose (%)	19.25

2. Materials and methods

2.1. Instruments: -

- 1-Atomic Absorption Spectrometer, Thermo Scientific, ICE 3000 Series, England.
- 2-pH meter model Thermo Scientific Orion 2-star, serial no.: b30555, USA.
- 3-Spectrophotometer Aquarius, CECIL CE7400S, serial 146-456, England.
- 4-Hot plate, Torrey pines hp11, Serial No.: 05051108, USA
- 5-Oven Medline, England.
- 6-Ball mill model PM400, England

Chemicals: -

All chemicals were used without further purification in all experiments. Aluminum Nitrate, Cadmium Sulfate octa hydrate, Lead acetate tri hydrate, Eriochrome cyanine R, Acetic acid, and 1,10-phenanthroline were purchased from Sigma-Aldrich, USA. Nitric acid, Ammonium acetate, and Sodium acetate were purchased from Panreac Quimica S.L.U. Ferric Chloride hexahydrate was purchased from POCh Gliwice, Poland. Hydrochloric acid was purchased from J.T. Baker, USA. Sodium hydroxide was purchased from Fluka.

2.2. Solutions

Aluminium (III) standard solution: Al (III) solution (10 ppm) was prepared in a volumetric flask by taking 10 ml of (1000 ppm) ready solution and completing it to 1000 ml. Ferric (III) standard solution: Fe (III) solution 1000 mg/L was made by dissolving (2.42 g) from Ferric Chloride hexahydrate ($\text{FeCl}_3 \cdot 6\text{H}_2\text{O}$) (MW 270.30 g) in 500 ml of distilled water, then standardized[17]. Lead (II) standard solution: Pb (II) solution 1000 mg/L was made by dissolving (0.9153 g) from Lead acetate trihydrate $\text{Pb}(\text{CH}_3\text{COO})_2 \cdot 3\text{H}_2\text{O}$ (MW 379.33g) in 500 ml of distilled water then standardized. Cadmium (II) standard solution: Cd (II) solution 1000 mg/L was made by dissolving (1.571 g) from Cadmium Sulfate octa hydrate ($\text{CdSO}_4 \cdot 8\text{H}_2\text{O}$) (MW 352g) in 500 ml of distilled water. then standardized according to[17]. Phenanthroline solution: 100 mg 1,10-phenanthroline monohydrate, $\text{C}_{12}\text{H}_8\text{N}_2 \cdot \text{H}_2\text{O}$, dissolved in 100 mL distilled water by stirring and heating to 80°C [18]. Eriochrome cyanine R solution: 150 mg weighed and dissolved in 50 mL distilled water. pH adjusted from about 9 to about 2.9 with 1:1 acetic acid and then completed with distilled water to 100 ml. Sodium acetate buffer solution: 136 g sodium acetate, $\text{CH}_3\text{COONa} \cdot 3\text{H}_2\text{O}$ weighed, dissolved in water, and then 40 mL 1N acetic acid was added and completed to 1 L. Ammonium acetate buffer solution: 250 g $\text{CH}_3\text{COONH}_4$ weighed and dissolved in 150 mL water. Then 700 mL of concentrated (glacial) 99.5 % acetic acid was added and diluted to 1 L[19].

2.3. Adsorbent preparation

One kilogram of persimmon leaves was collected from a persimmon farm in Faqous, Sharkia, Egypt. The persimmon leaves were washed several times with distilled water, then dried in air at room temperature for one week, then crushed with a blender, sieved 150 mesh sieve, and kept in a 250 ml plastic bottle. The Persimmon leaves were divided into five parts; four parts were dried at different temperatures (85,105,150, and 170°C) for two hours to form persimmon leaves powder sorbent, and the fifth part was converted to nano one.

2.4. General procedures

0.5 g of persimmon leaves powder was placed in five 100 ml conical flasks and mixed with 50 ml with a concentration of 6 mg/L of metal ions solutions which were studied and shaken for 30 minutes. Then filtration of the metal ions solution from the flask using filter paper. The concentration of each ion was measured by spectrophotometer for (Al, Fe) and Atomic Absorption spectrometer for (Pb, Cd).

2.5. Factors affecting the removal of Al (III), Fe (III), Pb (II), and Cd (II) from a different water sample

Effect of quantity of adsorbent

The impact of the quantity of adsorbent on the efficiency of absorption of both Al (III), Fe (III), Pb (II), and Cd (II) was studied. (0.1, 0.25, 0.5, 1.0, 1.5 g) of persimmon leaves powder placed in five conical flasks containing 50 ml of 6 mg/L metal ions solutions studied and shaken for 30 minutes. Then filter papers were used to filter it. Each ion concentration was measured by spectrophotometer for (Al, Fe) and Atomic Absorption spectrometer for (Pb, Cd).

Effect of pH

50 ml of the metal ion solution of Al (III), Fe (III), Pb (II), and Cd (II) were contacted with 0.5 g of the adsorbent in five conical flasks, and the pH of the solution was varied with 0.1M HCl and 0.1M NaOH to obtained pH of 1,3,5,7 and 9. The solution was stirred for 30 minutes; after filtration, each ion concentration was measured by spectrophotometer for (Al, Fe) and Atomic Absorption spectrometer for (Pb, Cd).

Effect of concentration of metal ions

The impact of the initial concentration of metal ions was studied. Different concentrations of the metal ions were prepared by serial dilution of the stock metal ion solution (2, 4, 6,8, and 10 mg/L) and then contacted with a fixed dosage (0.5 g) of the adsorbent and 50 ml of the metal ion solution for both Al (III), Fe (III), Pb (II) and Cd (II) in a flask, and shake for 30 min. Then the mixture was filtered and analyzed using a spectrophotometer and Atomic Absorption spectrometer.

Effect of contact time

Reaction time is a significant feature that influences how well heavy metals adsorb in a medium. The effect of time on the elimination of Al (III), Fe (III), Pb (II), and Cd (II) onto persimmon leaves powder was studied. Experiments were carried out to examine the effect after (5, 15, 30, 60, and 120 min) on the removal of Al (III), Fe (III), Pb (II), and Cd (II). 50 ml of 6 mg/L of the metal ion solution for Al (III), Fe (III), Pb (II), and Cd (II) were contacted with 0.5 g of the adsorbent in a flask and shaken for 30 minutes and then filtered using filter paper. Furthermore, concentration was measured as above.

Effect of foreign ion interference

The impact of foreign ion interference was studied by mixing 0.5 g Persimmon leaves powder with 50 ml from a series of solutions containing 6 mg/L Al (III) and 6mg/L of $[Na^+, k^+, Ca^{2+}, SO_4^{2-}, CO_3^{2-}, I^-]$ separately for Al (III). Furthermore, Fe (III) adsorbent was mixed with 50 ml from a series of solutions containing 6 mg/L Fe (III) and 6 mg/L of $[Na^+, k^+, Ca^{2+}, SO_4^{2-}, CO_3^{2-}, I^-]$ separately. Moreover, for Pb(II) adsorbent mixed with 50 ml from a series of solutions containing 6 mg/L Pb(II) and 6 mg/L of

$[Na^+, k^+, Ca^{2+}, SO_4^{2-}, CO_3^{2-}, I^-]$ separately, and for Cd(II) adsorbent mixed with 50 ml from series of solutions contain 6 mg/L Cd(II) and 6 mg/L of $[Na^+, k^+, Ca^{2+}, SO_4^{2-}, CO_3^{2-}, I^-]$ separately, in a flask, and shake for 30 minutes. Then filtered using filter paper. The concentration of ions is determined using a spectrophotometer and atomic absorption spectrometer.

2.6. Applications

Removal of Pb(II) and Cd (II) from the water samples from Bahr Elbaqar at Faqous, Sharkia, Egypt, and groundwater using Persimmon leaves adsorbent two liters of sewage water. Two liters of groundwater and wastewater were collected and boiled to 250 ml separately, then 50 ml of each sample was added to 0.5 g of Persimmon leaves powder and shaken for 30 minutes, then filtered using filter paper and the concentration of Pb (II), and Cd (II) was determined using atomic absorption spectrometer.

2.7. Nano persimmon leaves powder

Conversion of Persimmon leaves powder to nano persimmon leaves powder.

The fifth part of the Persimmon leaves powder was dried at 170 °C for 2 hours. Then a 10 g form of Persimmon leaves powder is ground in a Ball mill device to convert persimmon leaves powder to a particular nano size.

General procedures for removal of heavy metals using nano persimmon leaves powder

0.1 g of nano Persimmon leaves powder was placed in five conical flasks and mixed with 50 ml metal ions solutions which were studied and shaken for 30 minutes. Then filtration of the metal ions solution from the flask using filter paper. Then atomic absorption spectroscopy was used to calculate each ion's concentration.

3. RESULTS AND DISCUSSION

Characterization of the Persimmon leaves adsorbent and nano persimmon leaves powder.

The characterization of persimmon powder was studied using FTIR spectra, the results of which are given in Fig. 1. The peaks at 3383 cm^{-1} and 1340 cm^{-1} in the spectrum of persimmon powder are attributed to O-H stretching vibration and O-H bending, the weak peak at 1695 cm^{-1} and the sharp peak at 1614 cm^{-1} are attributed to C=O stretching vibrations of ester and ketone groups. The peaks at 1239 cm^{-1} are attributed to C=C-O stretching. Peaks in the 850-740 cm^{-1} range

can be linked to deformation vibrations at the C-H bond in phenolic rings [20].

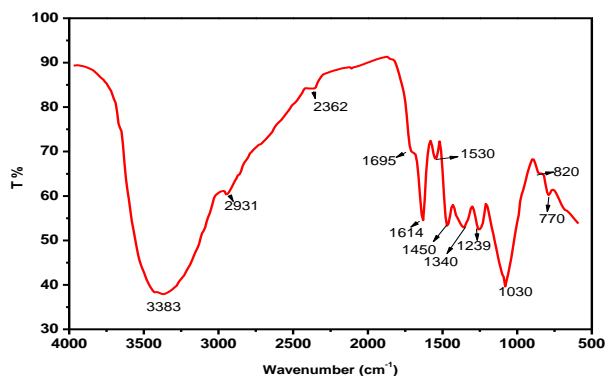


Figure (1): FTIR spectrum of normal Persimmon leaves powder

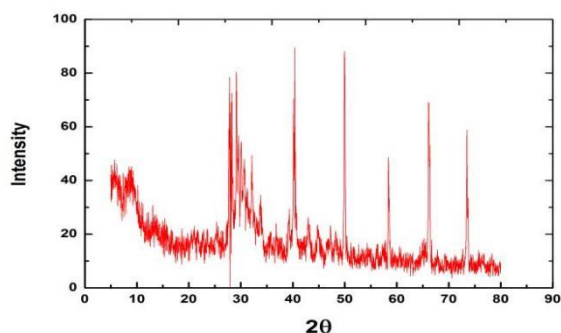


Figure (2): XRD of nano Persimmon powder

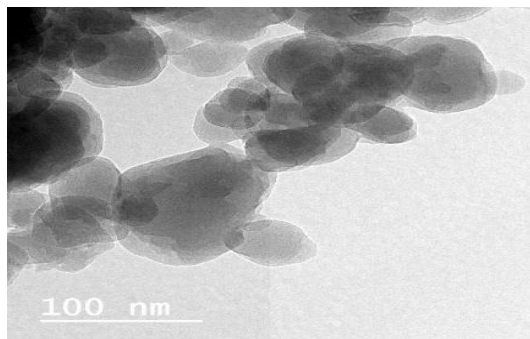


Figure (3): TEM images for nano Persimmon leaves powder

Nano persimmon leaves powder particle size is proved by the XRD technique; the XRD pattern affects the particle sizes to smaller sizes which can be calculated by Scherer's equation.

$$\text{Scherer's equation: } D = K \lambda / \beta \cos \theta \quad (1)$$

Where: λ is the wavelength of X-Ray (0.1540 nm), β is FWHM (full width at half maximum), and θ is the diffraction angle; the particles sizes were found to be in the range of between 25-30 nm at the more intense x-ray beaks at 28.1°, 40.8.0° and 50°.

During the study of the adsorption process on Persimmon powder, many parameters influence heavy

metal removal from aqueous solutions. These include drying temperature, Persimmon leaves quantity, pH, contact time, starting metal ion concentration, and foreign ion interference.

Effect of drying temperature

The drying temperature of persimmon leaves was regarded as one of the essential factors affecting adsorption efficiency; as shown in Fig. 4, it was found that the best drying temperature is 105, 150, 105, 105 °C for Al (III), Fe (III), Pb (II), and Cd (II) respectively.

Effect of amount of persimmon leaves

Adsorbent dosage effects on adsorption of Al (III), Fe (III), Pb (II), and Cd (II) were studied; as shown in Fig. 5, it was found that the best amount of persimmon leaves is 1, 0.25, 0.5, 0.5 g for Al (III), Fe (III), Pb (II), and Cd (II) respectively.

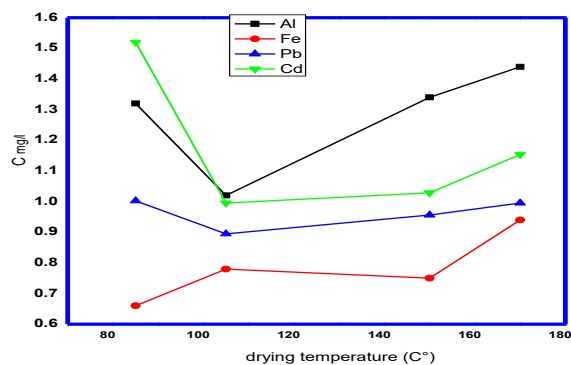


Figure (4): effect of drying temperature on normal Persimmon leaves powder

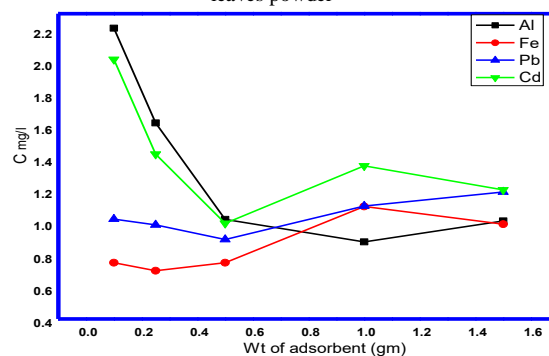


Figure (5): effect of the amount of normal Persimmon leaves powder . Effect of pH

One of the significant features influencing the sorption of metal ions is pH. The ability of hydrogen ions to compete with metal ions for the active sites on the sorbent surface depends directly on differences in initial pH. The impact of pH on the sorption of Al (III), Fe (III), Pb (II), and Cd (II) ions onto persimmon leaves was studied at pH (1,3,5,7,9); as shown in Fig. 6, it was

found that the best pH is 9 for Al (III), Fe (III), Pb (II), and Cd (II) respectively.

3.4. Effect of metal ion concentration

The impact of initial concentrations on the removal of Al (III), Fe (III), Pb (II), and Cd (II) ions by persimmon leaves was studied. As shown in Fig. 7, it was found that the best initial concentration is 2 mg/L for Al (III), Fe (III), Pb (II), and Cd (II), respectively.

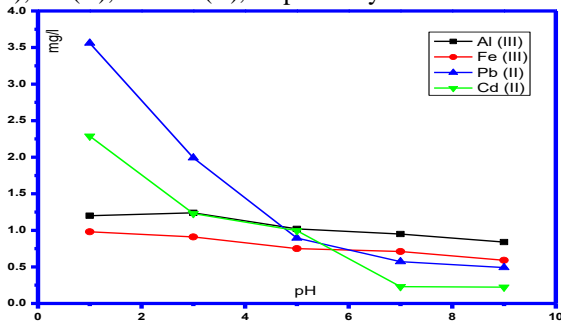


Figure (6): effect of pH on heavy metal removal by normal Persimmon leaves powder

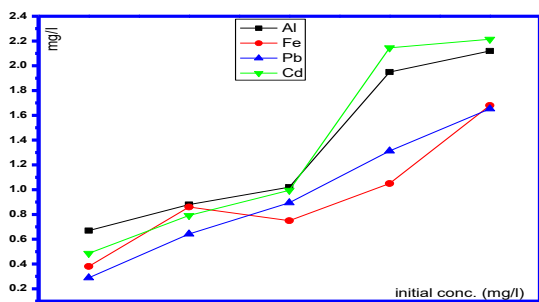


Figure (7): effect of initial concentration

Effect of contact time

The impact of time on the adsorption process was examined to determine the equilibrium point. The experiments were carried out to detect the impact of contact time on the removal of Al (III), Fe (III), Pb (II), and Cd (II) ions; as shown in Fig. 8, it was found that the best time is 15, 30, 60, 120 minutes for Al (III), Fe (III), Pb (II), and Cd (II) respectively.

Effect of foreign ion interference

The impact of foreign ion interference on adsorption Al (III), Fe (III), Pb (II), and Cd (II) by persimmon leaves were found.

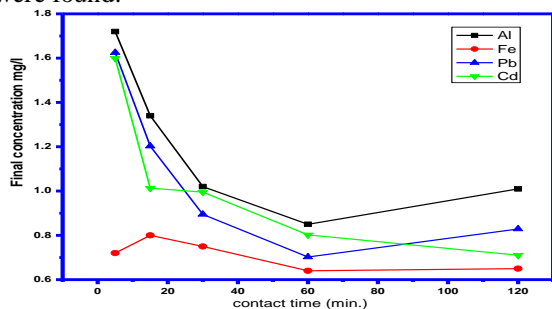


Figure (8): effect of contact time with normal Persimmon leaves powder

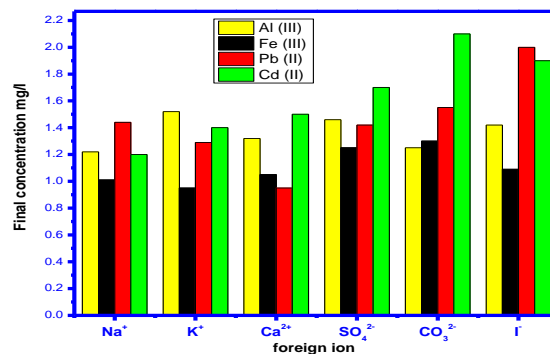


Figure (9): effect of foreign ion interferences

Nano persimmon leaves powder results Factors affecting removal of Pb (II) and Cd (II) by nano persimmon leaves powder sorbent.

Effect of quantity of nano persimmon leaves powder

The quantity of nano persimmon leaves powder impact on the efficient absorption of both Pb (II) and Cd (II) was studied. (0.05, 0.075, 0.1, 0.125, 0.15 g) of persimmon leaves powder placed in five conical flasks containing 50 ml of 6 mg/L metal ions solutions which were studied and shaken for 30 minutes. They were then filtered using filter paper. The concentration of each ion was measured using an Atomic Absorption spectrometer; as shown in Fig. 10, it was found that the best amount of nano persimmon leaves is 0.15g, 0.075g for Pb (II), and Cd (II), respectively.

Effect of contact time

The impact of contact time on the uptake of Pb (II) and Cd (II) ions onto nano persimmon leaves powder was studied. Experiments were carried out to investigate the impact of different contact times (5,15,30,60, and 120 min) on the removal of Pb (II) and Cd (II), 50 ml of the metal ion solution. Pb (II) and Cd (II) were contacted with 0.1 g of the adsorbent in a flask, shaken for 30 minutes, and filtered with filter paper. Atomic Absorption Spectrometers were used to measure the concentration of Pb (II) and Cd (II); as shown in Fig. 11, it was found that the best time was 60, 30 minutes for Al (III), Fe (III), Pb (II), and Cd (II) respectively.

Effect of initial metal ions concentration

The impact of the initial concentration of metal ions was studied. Different concentrations of the metal ions were prepared by serial dilution of the stock solution (2, 4, 6,8, and 10 mg/L) and then contacted with a fixed dosage of the adsorbent and 50 ml of the metal ion solution for both Pb (II) and Cd (II) a flask, and shake for 30 minutes then filtered with filter paper. Atomic Absorption Spectrometers were used to measure the concentration of Pb (II) and Cd (II); as shown in Fig. 12, it was found that the best initial concentration is 2 mg/L, 6 mg/L for Pb (II), and Cd (II) respectively.

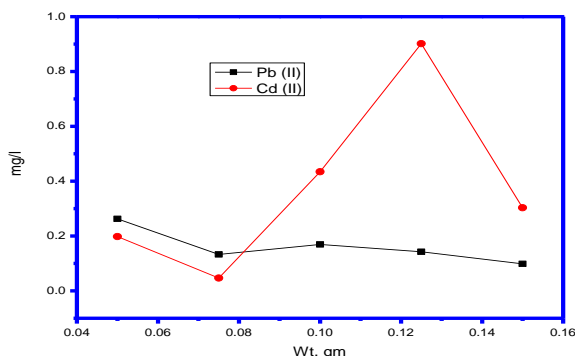


Figure (10): effect of the amount of nano persimmon

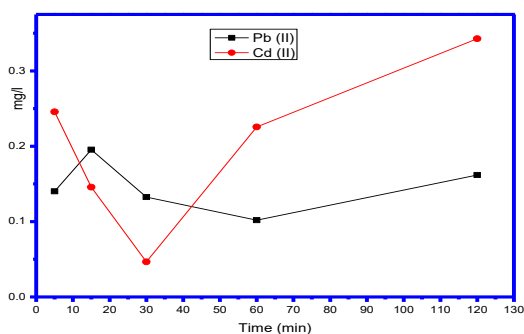


Figure (11): effect of contact time with nano persimmon

Table 2,3,4 shows that using nano persimmon leaves powder is more effective than normal Persimmon leaves in Pb^{2+} and Cd^{2+} removal even if using the amount of nano persimmon leaves powder is smaller than normal Persimmon leaves powder.

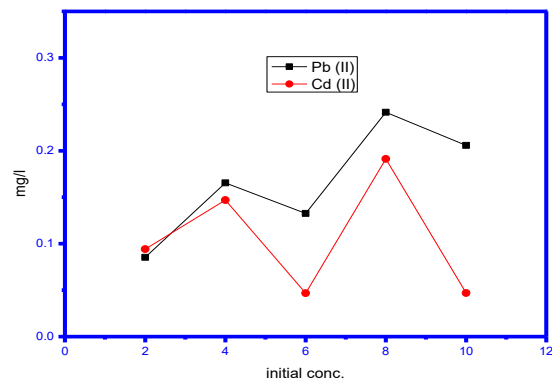


Figure (12): effect of initial concentration with nano persimmon

Comparison between Normal DPL and Nano DPL results

Effect of initial concentration.

Table (2): compares the effect of initial concentration on removing Pb and Cd using normal Persimmon leaves powder and nano Persimmon leaves powder.

C_{int}	Pb (II) mg/L				Cd (II) mg/L			
	Normal DPL		Nano DPL		Normal DPL		Nano DPL	
	C_{eq}	% Re	C_{eq}	% Re	C_{eq}	% Re	C_{eq}	% Re
2	0.2885	85.58	0.0854	95.73	0.4855	75.73	0.0941	95.30
4	0.6421	83.95	0.1655	95.86	0.7921	80.20	0.1469	96.33
6	0.8945	85.09	0.1326	97.79	0.9952	83.41	0.0467	99.22
8	1.3129	83.59	0.2414	96.98	2.1453	73.18	0.1913	97.61
10	1.6521	83.48	0.2058	97.94	2.214	77.86	0.0469	99.53

Effect of the contact time.

Table (3) compares the effect of contact time on removing Pb and Cd using normal Persimmon leaves to powder and nano Persimmon leaves powder.

Time (min)	Pb (II) mg/L				Cd (II) mg/L			
	$C_{int}=6$				$C_{int}=6$			
	Normal DPL		Nano DPL		Normal DPL		Nano DPL	
	C_{eq}	% Re	C_{eq}	% Re	C_{eq}	% Re	C_{eq}	% Re
5	1.0215	82.98	0.1402	97.66	1.5992	73.35	0.2458	95.90
15	0.9852	83.58	0.1954	96.74	1.0128	83.12	0.1457	97.57
30	0.8945	85.09	0.1326	97.79	0.9952	83.41	0.0467	99.22
60	1.1028	81.62	0.1019	98.30	0.8023	86.63	0.2256	96.24
120	1.1905	80.16	0.1618	97.30	0.7104	88.16	0.3427	94.29

Effect of amount of persimmon leaves.

Table (4) compares the effect of the amount of Persimmon leaves on removing Pb and Cd using normal Persimmon leaves to powder and nano persimmon leaves powder.

Wt. g	Pb (II) mg/L		Cd (II) mg/L		Wt. g	Pb (II) mg/L		Cd (II) mg/L	
	C _{int} =6		C _{int} =6			C _{int} =6		C _{int} =6	
	Normal DPL		Normal DPL			Nano DPL		Nano DPL	
	C _{eq}	% Re	C _{eq}	% Re		C _{eq}	% Re	C _{eq}	% Re
0.1	1.02	82.98	1.59	73.35	0.05	0.26	95.63	0.19	96.70
0.25	0.98	83.58	1.01	83.12	0.075	0.13	97.79	0.04	99.22
0.5	0.89	85.09	0.99	83.41	0.1	0.16	97.18	0.43	92.76
1	1.10	81.62	0.80	86.63	0.125	0.14	97.63	0.90	84.98
1.5	1.19	80.16	0.71	88.16	0.15	0.09	98.36	0.30	94.95

Adsorption isotherm for Al (III), Fe (III), Pb (II), and Cd (II) using normal persimmon leaves

Adsorption efficiency is determined by the chemical and physical characteristics of the adsorbents. This research examined four different adsorption isotherms (Langmuir, Freundlich, Temkin, and Dubinin-Radushkevich) for Al, Fe, Pb, and Cd on powdered persimmon leaves.

Langmuir Adsorption Isotherm

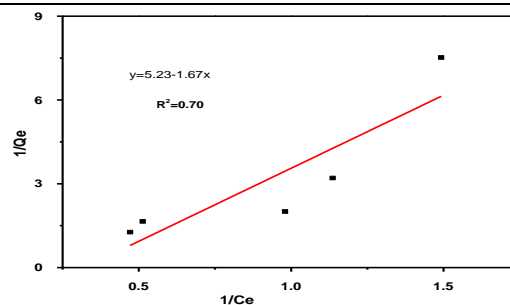
Langmuir provides a quantitative description of creating a monolayer adsorbate on the adsorbent's outer surface [21]. Langmuir presented the following equation.

$$q_e = \frac{Q_0 K_L C_e}{1 + K_L C_e} \dots\dots\dots 2$$

Where: C_e= the concentration at the equilibrium of adsorbate (mg/L), q_e= the metal quantity adsorbed at equilibrium per gram of adsorbent (mg/g), Q₀ = the maximum capacity of coverage of a single layer (mg/g), and K_L = constant of Langmuir (L/mg). The slope and intercept of the Langmuir plot of 1/q_e vs. 1/C_e were used to get the values of q_{max} and K_L[22]. The equilibrium parameter R_L, also known as the separation factor or equilibrium parameter, is a dimensionless constant that can be used to define the fundamental characteristics of the Langmuir isotherm. [23].

$$R_L = \frac{1}{1 + K_L C_0} \dots\dots\dots 3$$

C₀ = initial concentration and K = (Langmuir Constant) [21]. Figs. 13,14,15 and 16 represent Langmuir Adsorption Isotherm for Al, Fe, Pb, and Cd, respectively.



Figure(13):Langmuir isotherm for adsorption of Al(III)

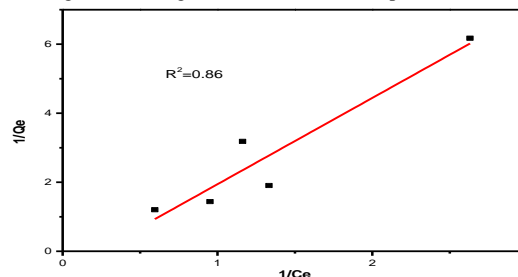
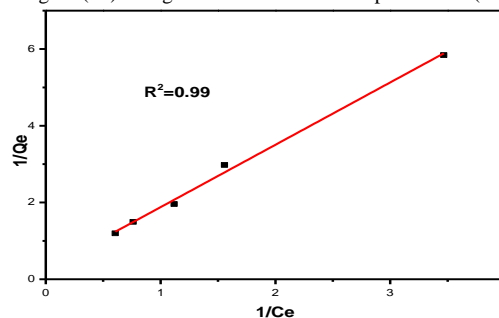


Figure (14): Langmuir isotherm for adsorption of Fe (III)



Figure(15):Langmuir isotherm for adsorption ofPb

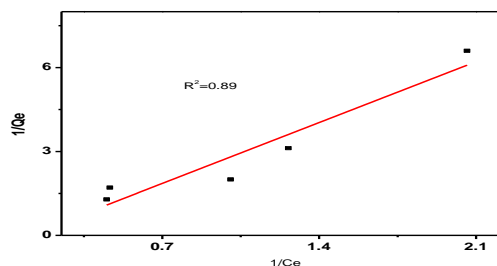


Figure (16): Langmuir isotherm for adsorption of Cd (II)

Freundlich Adsorption Isotherm

Freundlich is a popular way to describe how the heterogeneous surface adsorbs substances [24]. These data frequently match the empirical formula suggested by Freundlich:

$$Q_e = K_f C_e^{\frac{1}{n}} \dots\dots\dots 4$$

Where Q_e = the metal quantity adsorbed at equilibrium per gram of adsorbent (mg/g), K_f = Freundlich constant (mg/g), C_e = the adsorbate concentration at equilibrium (mg/L), n = intensity of adsorption. By Linearizing equation 4, we have:

$$\log Q_e = \log K_f + \frac{1}{n} \log C_e \dots\dots\dots 5$$

Figs. 17,18,19 and 20 represent Freundlich Adsorption Isotherm for Al, Fe, Pb, and Cd, respectively.

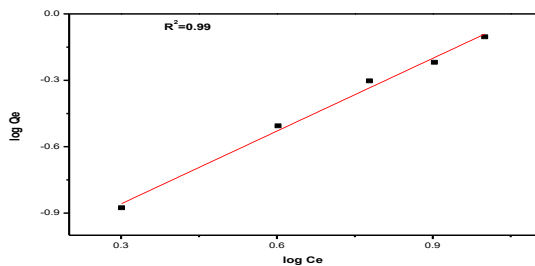


Figure (17): Freundlich isotherm for adsorption of Al(III)

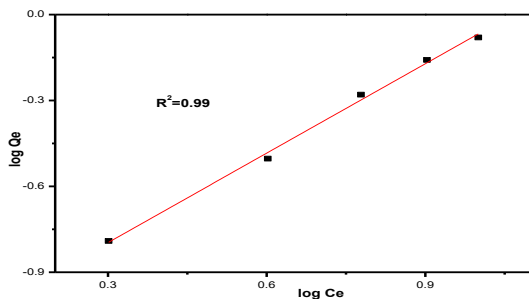


Figure (18): Freundlich isotherm for adsorption of Fe(III)

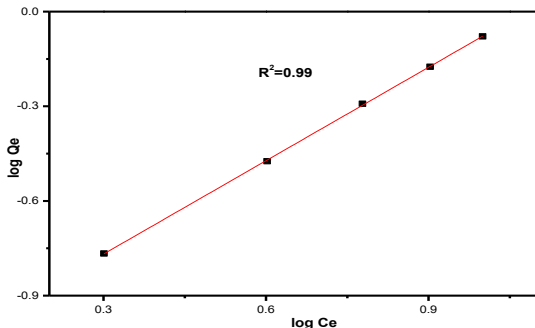


Figure (19): Freundlich isotherm for adsorption of Pb (II)

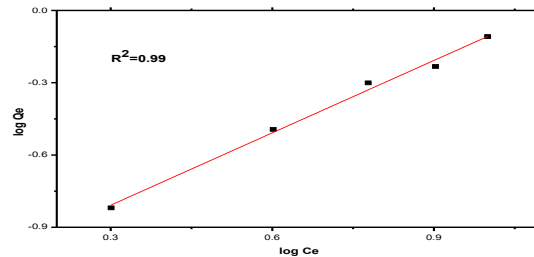


Figure (20): Freundlich isotherm for adsorption of Cd (II)

It is observed from Figs. 13- 20 the value of R^2 in Freundlich isotherm for Al, Fe, Pb, and Cd were higher than that produced from Langmuir isotherm; also, it is closer to the unit assumed that the adsorption process is fitted to Freundlich isotherm.

Temkin Isotherm

This isotherm has a part that explicitly considers how the adsorbate and adsorbent interact. By ignoring the extremely low and high concentration values, the model supposes that the function of the temperature of all molecules in the layer will decrease linearly rather than logarithmically with coverage [25]. The constants were determined from the slope and intercept of a plot of the variable sorbed q_e against $\ln C_e$. The equation implies that the derivation's binding energies are distributed uniformly (up to some maximal binding energy). The following equation [26] provides the model.

$$q_e = \frac{RT}{b} \ln(A_T C_e) \dots\dots\dots 6$$

$$q_e = \frac{RT}{b_T} \ln A_T \left(\frac{RT}{b}\right) \ln C_e \dots\dots\dots 7$$

$$B = \frac{RT}{b_T} q_e = B \ln A_T + B \ln C_e \dots\dots\dots 8$$

A_T = binding constant of Temkin isotherm at equilibrium (L/g), b_T = constant of Temkin isotherm, R = gas constant (8.314J/mol/K), T = absolute temperature at 298K, and B = heat of sorption constant (J/mol). Figs. 21,22,23 and 24 represent Temkin Adsorption Isotherm for Al, Fe, Pb, and Cd, respectively.

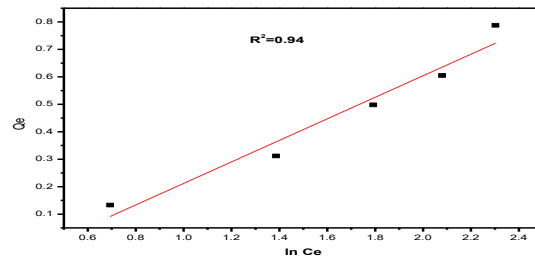


Figure (21): Temkin isotherm for adsorption of Al (III)

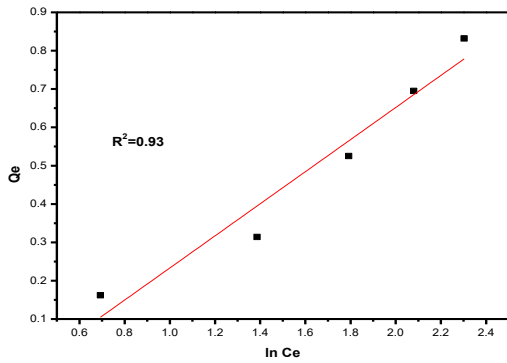


Figure (22): Temkin isotherm for adsorption of Fe (III)

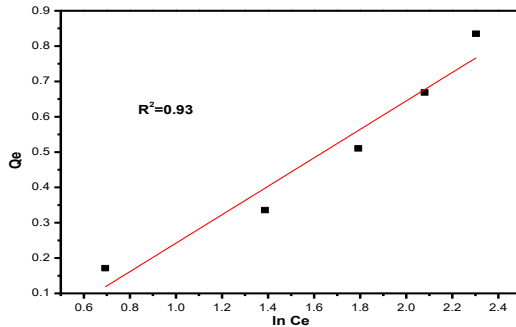


Figure (23): Temkin isotherm for adsorption of Pb (II)

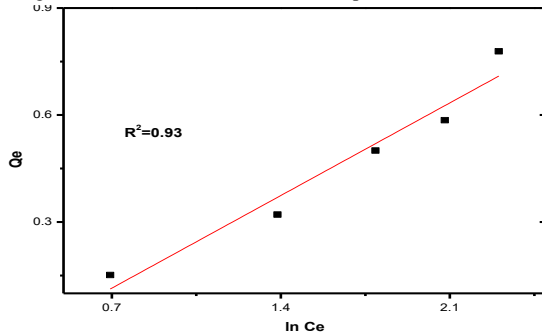


Figure (24): Temkin isotherm for adsorption of Cd (II)

Dubinin–Radushkevich isotherm model

Dubinin-Radushkevich isotherm is frequently used to explain the adsorption mechanism with a Gaussian energy distribution onto a heterogeneous surface [21]. The data from the intermediate range of concentrations and high solute activity have been impacted positively by the model on numerous occasions.

$$q_e = (q_s) \exp(-K_{ad}\epsilon^2) \dots\dots\dots 9$$

$$\ln q_e = \ln(q_s) - (K_{ad}\epsilon^2) \dots\dots\dots 10$$

qe is the equilibrium quantity of adsorbate in the adsorbent (mg/g), qs= theoretical saturation capacity (mg/g); K_{ad} = isotherm constant (mol²/kJ²), and ε= isotherm constant of Dubinin–Radushkevich. The method was frequently used to differentiate between the chemical and physical adsorption of ions with its mean free energy, E per

molecule of adsorbate can be calculated by the relationship [26].

$$E = \left[\frac{1}{\sqrt{2B_{DR}}} \right] \dots\dots\dots 11$$

Where B_{DR} stands for the constant of isotherm, ε can be calculated as

$$\epsilon = RT \ln \left[1 + \frac{1}{C_e} \right] \dots\dots\dots 12$$

R = gas constant (8.314 J/mol K), C_e = equilibrium concentration of adsorbate (mg/L), and T= absolute temperature (K), The model Dubinin–Radushkevich (DRK) has some unique characteristics, one of which is that it is temperature-dependent. Adsorption data at various temperatures are displayed against the logarithm of the amount adsorbed (ln q_e) vs ε² the square of potential energy. Figs. 25,26,27 and 28 represent Dubinin–Radushkevich Adsorption Isotherm for Al, Fe, Pb, and Cd, respectively.

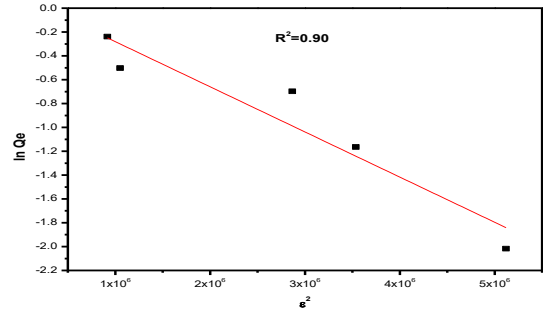


Figure (25): Dubinin isotherm for adsorption of Al (III)

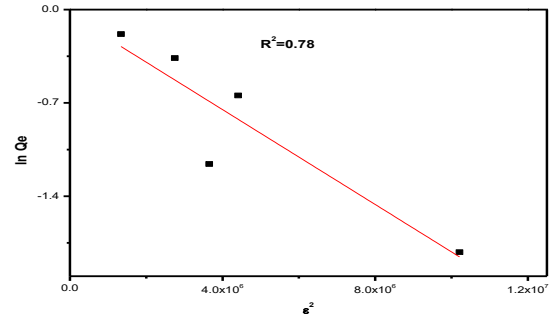


Figure (26): Dubinin isotherm for adsorption of Fe (III)

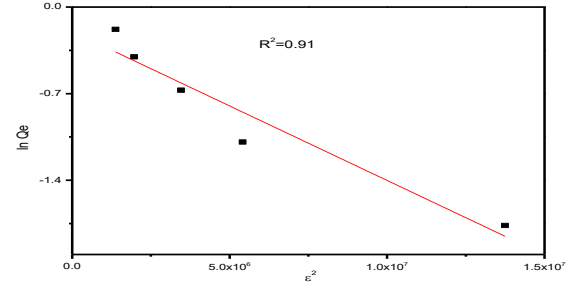


Figure (27): Dubinin isotherm for adsorption of Pb(II)

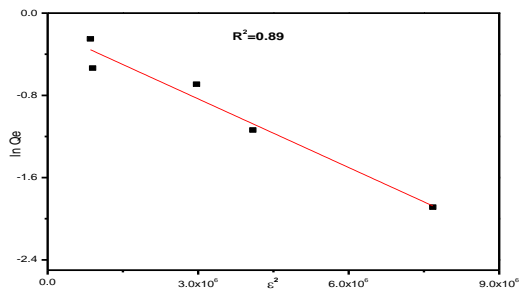


Figure (28): Dubinin isotherm for adsorption of Cd (II)

It is observed from Figs. 21- 28 the value of R^2 in Temkin isotherm for Al, Fe, Pb, and Cd were higher than that produced from Dubinin–Radushkevich isotherm; also, it is closer to the unit assumed that the adsorption process is fit to Temkin isotherm.

Adsorption Kinetic:

Pseudo First-Order:

Pseudo first-order was used to investigate the kinetics of the adsorption of Al (III), Fe (III), Pb (II), and Cd (II) on Persimmon leaves by plotting $\ln(q_e - q_t)$ vs. time(t), which results in a straight line as shown in Figs. 29,30,31 and 32. The intercept and slope of the linear regressions were used to compute the rate constant K_f (1/min) and q_e . The correlation coefficient (R^2) values are low, and the values of q_e estimated from the linear plots do not agree with the experimental data, which proves that pseudo-first-order kinetics is not used in the adsorption of Al (III), Fe (III), Pb (II), and Cd (II) on Persimmon leaves .

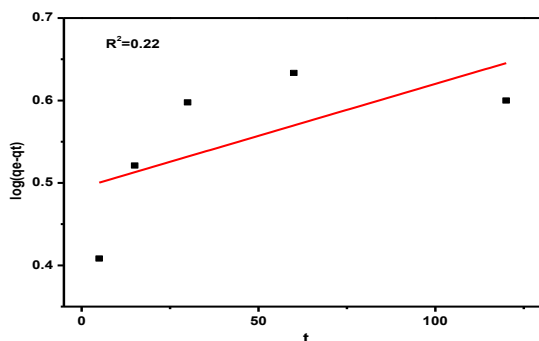
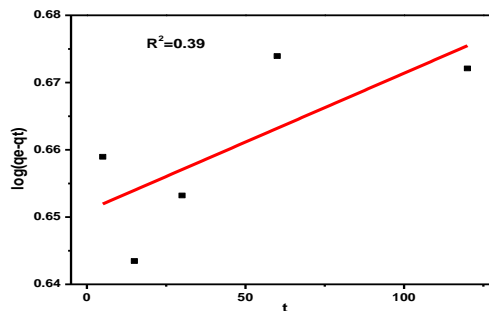


Figure (29): Pseudo-first-order Kinetic for Al (III)



Figure(30):Pseudo-first-order Kinetic for Fe(III)

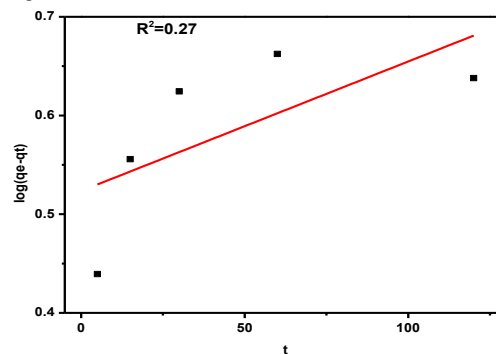


Figure (31): Pseudo-first-order Kinetic for Pb (II)

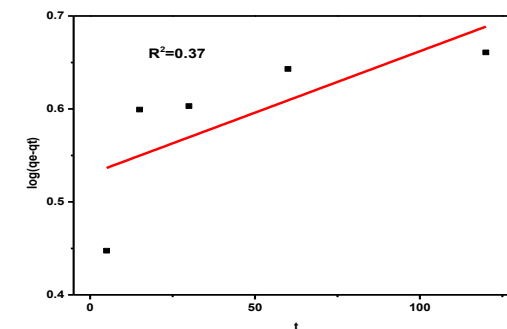


Figure (32): Pseudo-first-order Kinetic for Cd (II)

Pseudo Second-Order:

Plotting t/qt versus t results in a straight line, as seen in Figs. 33,34,35 and 36 were used to examine the applicability of the pseudo-second-order kinetics model. The slope and intercept can be used to estimate the values of $1/q_e$ and $1/ksq_e$, respectively. The correlation coefficient for the pseudo-second-order kinetic model was greater than that of the pseudo-first-order kinetic model for persimmon leaves, and the value of q_e produced from the pseudo-second-order model has shown that the q_e values are incredibly near to the experimental values. The experimental findings are consistent with the pseudo-second-order equation compared to the pseudo-first-order equation, as shown by the high correlation coefficient ($R^2 = 1.0$). The possibility that the adsorption process is

chemisorption can be inferred from this. That demonstrates that the adsorption coincides with the pseudo-second-order reaction, and the chemisorption process appeared to be in control of the adsorption of Al (III), Fe (III), Pb (II), and Cd (II).

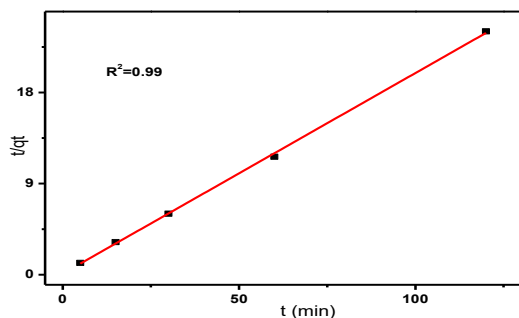


Figure (33): Pseudo-Second-Order Kinetic for Al (III)

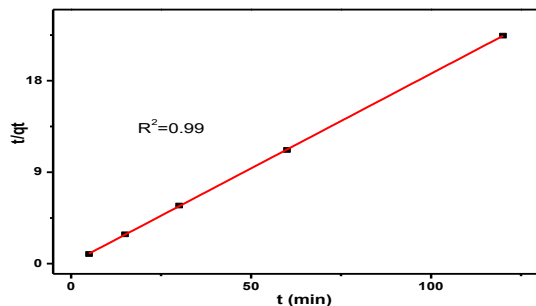


Figure (34): Pseudo-Second-Order Kinetic for Fe (III)

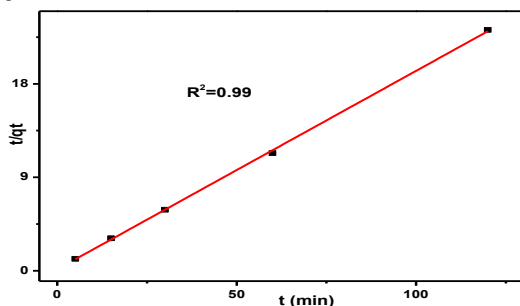


Figure (35): Pseudo Second Order Kinetic for Pb (II)

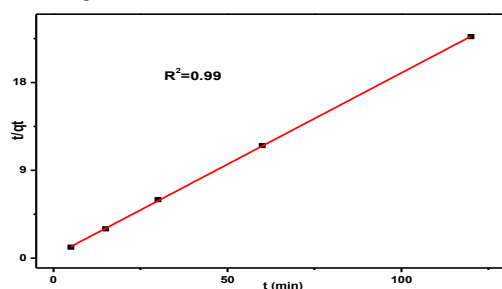


Figure (36): Pseudo Second Order Kinetic for Cd (II)

The R^2 of the second-order kinetic model was greater than that of the first-order kinetic model for Al^{3+} , Fe^{3+} , Pb^{2+} , and Cd^{2+} , signifying that the pseudo-second-order is better fitted than the

pseudo-first-order model and implies that the sorption completely conforms to second-order reaction. Consequently, the sorption process for Al^{3+} , Fe^{3+} , Pb^{2+} , and Cd^{2+} seemed to be dominated by a chemisorption mechanism [29].

Intra-Particle Diffusion Model:

Intra-particle diffusion model was utilized to explain further the mechanism of Fe (III), Al (III), Pb (II), and Cd (II) removal by Persimmon leaves. The possibility of intraparticle diffusion was examined by using the Intra-particle diffusion model [30]. The influence of the boundary layer increases with increasing intercept [31]. The constant rate k_{id} is calculated using the slope of the linear parts of the diagram of the sorbed amount vs. the $t^{0.5}$.

Intraparticle diffusion is the only rate-controlling step when q_t versus $t^{0.5}$ is shown linearly and if the line crosses the origin. If not, other mechanisms are also concerned. The plots q_t versus $t^{0.5}$ did not pass through the origin as shown in Figs. 37,38,39 and 40. indicating that although intraparticle diffusion played a factor in the adsorption process, it was not the only factor in rate regulation.

The positive value of intercept C suggests some boundary layer control [30]; additionally, the lower values of the intraparticle diffusion model's R^2 for persimmon leaves suggest that the model was not the sole factor influencing the rate.

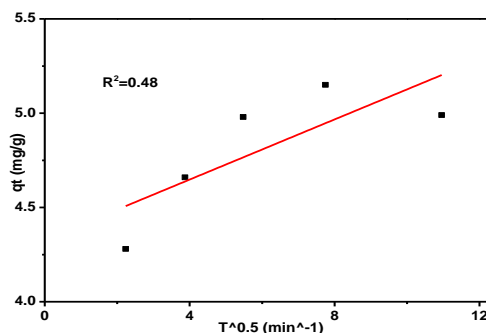
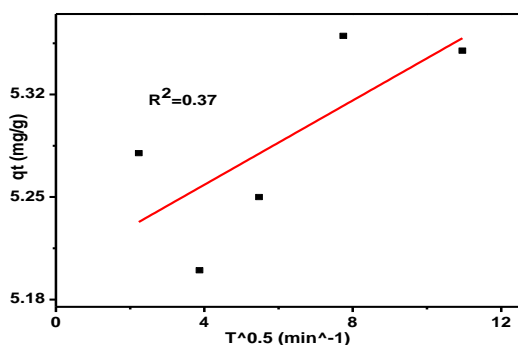


Figure (37): Intraparticle diffusion graph for Al (III)



Figure(38): Intraparticle diffusion graph for Fe (III)

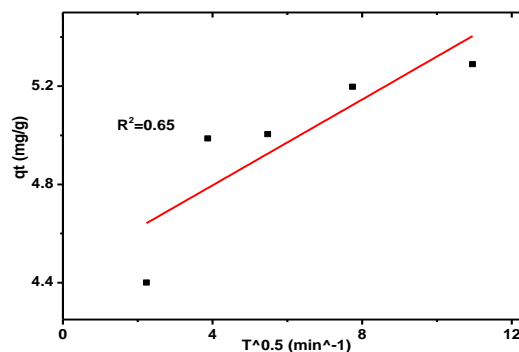


Figure (40): Intraparticle diffusion graph for Cd (II)

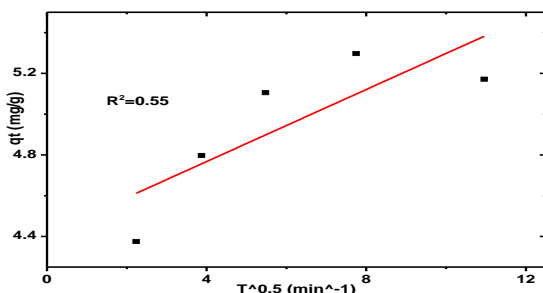


Figure (39): Intraparticle diffusion graph for Pb (II)

Statistical treatment

Table (5): Statistical analysis of Persimmon leaves on Al^{3+} , Fe^{3+} , Pb^{2+} , and Cd^{2+}

Parameter	Mathematical formula	Results			
		Al^{3+}	Fe^{3+}	Pb^{2+}	Cd^{2+}
Mean Value (\bar{X})	$\bar{X} = \sum (X_i / n)$	1.012	0.755	0.893	0.992
Standard deviation (SD)	$SD = \sqrt{\frac{\sum (X_i - \bar{X})^2}{n-1}}$	0.019321	0.01715	0.01767	0.01619
Relative Standard deviation (RSD%)	$RSD \% = (SD/\bar{X}) * 100$	1.909272	2.27276	1.97870	1.63238
Standard error of the mean (SEM)	$SEM = SD/\sqrt{n}$	0.006110	0.00542	0.00558	0.00512
Limit of detection (LOD)	$LOD = 3.3(SD/K)$	0.064082	0.05690	0.05860	0.05370
Limit of quantification (LOQ)	$LOQ = 10(SD/K)$	0.194189	0.17245	0.17758	0.16274
Student t-test	$t\text{-test} = ((\bar{X} - \mu) \sqrt{n}) / SD$	0.98198	0.92146	0.53688	0.39057

\bar{X} is the mean, SD is the standard deviation, and n is the sample size.

Conclusions

Batch experiments were carried out to remove Al, Fe, Pb, and Cd heavy metals from an aqueous solution with dried Persimmon leaves powder and nano Persimmon leaves powder. Moreover, according to the FT-IR analysis, DPL had a structure that facilitates heavy metal adsorption because it has Carboxylic groups, C=O carbonyl groups, CH stretching, O-H carboxylic acid, and bonded -OH groups. From experimental results, we understand that dried Persimmon leaves are an efficient, inexpensive, and commercially applicable new eco-friendly adsorbent for eliminating heavy

metal ions from contaminated water. Nano persimmon leaves powder is more effective than normal Persimmon leaves in Pb^{2+} and Cd^{2+} removal even if using the amount of nano persimmon leaves powder is smaller than normal Persimmon leaves powder. In addition, bio-adsorbent dried Persimmon leaves powder is very economical and could be used as a low-cost alternative to commercial activated carbon to eliminate heavy metal ions from wastewater.

Conflicts of interest

There are no conflicts to declare

Reference

- Rajendran S, Priya TAK, Khoo KS, Hoang TKA, Ng H-S, Munawaroh HSH, et al. A critical review on various remediation approaches for heavy metal contaminants removal from contaminated soils. *Chemosphere*. 2022;287:132369. <https://doi.org/10.1016/j.chemosphere.2021.132369>.
- Mohmand J, Eqani SAMAS, Fasola M, Alamdar A, Mustafa I, Ali N, et al. Human exposure to toxic metals via contaminated dust: Bio-accumulation trends and their potential risk estimation. *Chemosphere*. 2015;132:142–51. <https://doi.org/10.1016/j.chemosphere.2015.03.004>.
- Engwa GA, Ferdinand PU, Nwalo FN, Unachukwu MN. Mechanism and health effects of heavy metal toxicity in humans. *Poisoning Mod world-new tricks an old dog*. 2019;10:70–90.
- Peng H, Guo J. Removal of chromium from wastewater by membrane filtration, chemical precipitation, ion exchange, adsorption electrocoagulation, electrochemical reduction, electro dialysis, electro deionization, photocatalysis, and nanotechnology: a review. *Environ Chem Lett*. 2020;18:2055–68. <https://doi.org/10.1007/s10311-020-01058-x>.
- Sajid M, Nazal MK, Baig N, Osman AM. Removal of heavy metals and organic pollutants from water using dendritic polymers based adsorbents: a critical review. *Sep Purif Technol*. 2018;191:400–23. <https://doi.org/10.1016/j.seppur.2017.09.011>.
- Vakili M, Deng S, Cagnetta G, Wang W, Meng P, Liu D, et al. Regeneration of chitosan-based adsorbents used in heavy metal adsorption: A review. *Sep Purif Technol*. 2019;224:373–87. <https://doi.org/10.1016/j.seppur.2019.05.040>.
- Karnib M, Kabbani A, Holail H, Olama Z. Heavy metals removal using activated carbon, silica, and silica activated carbon composite. *Energy Procedia*. 2014;50:113–20. <https://doi.org/10.1016/j.egypro.2014.06.014>.
- Kluge RA, Tessmer MA. Caqui—Diospyros kaki. In: *Exotic Fruits*. Elsevier; 2018. p. 113–9. <https://doi.org/10.1016/B978-0-12-803138-4.00016-2>.
- Pangeni B, Paudyal H, Inoue K, Ohto K, Kawakita H, Alam S. Preparation of natural cation exchanger from persimmon waste and its application for the removal of cesium from water. *Chem Eng J*. 2014;242:109–16. <https://doi.org/10.1016/j.cej.2013.12.042>.
- Lee S-Y, Choi H-J. Persimmon leaf bio-waste for adsorptive removal of heavy metals from aqueous solution. *J Environ Manage*. 2018;209:382–92. <https://doi.org/10.1016/j.jenvman.2017.12.080>.
- Peralta-Videa JR, Lopez ML, Narayan M, Saube G, Gardea-Torresdey J. The biochemistry of environmental heavy metal uptake by plants: implications for the food chain. *Int J Biochem Cell Biol*. 2009;41(8–9):1665–77. <https://doi.org/10.1016/j.biocel.2009.03.005>.
- Emamverdian A, Ding Y, Mokhberdorran F, Xie Y. Heavy metal stress and some mechanisms of plant defense response. *Sci World J*. 2015;2015. <https://doi.org/10.1155/2015/756120>.
- Pu F, Ren X-L, Zhang X-P. Phenolic compounds and antioxidant activity in fruits of six *Diospyros kaki* genotypes. *Eur Food Res Technol*. 2013;237:923–32. <https://doi.org/10.1007/s00217-013-2065-z>.
- Singla RK, Dubey AK, Garg A, Sharma RK, Fiorino M, Ameen SM, et al. Natural polyphenols: Chemical classification, definition of classes, subcategories, and structures. Vol. 102, *Journal of AOAC International*. Oxford University Press; 2019. p. 1397–400. <https://doi.org/10.5740/jaoacint.19-0133>.
- Singh S, Joshi H. *Diospyros kaki* (Ebenaceae): a review. *Asian J Res Pharm Sci*. 2011;1(3):55–8.
- Abdelaleem M, Al-Sayed HMA, Elkhatry HO. Chemical, Technological and Biological Evaluation of Mulberry and Persimmon Leaves. *Arab J Nucl Sci Appl*. 2019;52(4):45–63. <https://doi.org/10.21608/ajnsa.2019.5487.1126>.
- Rice EW, Bridgewater L, Association APH. Standard methods for the examination of water and wastewater. Vol. 10. American public health association Washington, DC; 2012.
- Shukor MY, Syed MA, Raslan SA, Ithnin K, Shamaan NA, Syed MA. An iron determination method for azo dyes-contaminated wastewater. *Bull Environ Sci Sustain Manag* (e-ISSN 2716-5353). 2013;1(1):5–10. <https://doi.org/10.54987/bessm.v1i1.20>.

19. Singh U, Praharaj CS. Practical manual-chemical analysis of soil and plant samples. ICAR-Indian Inst Pulses Res Kanpur, Uttar Pradesh, India. 2017;
20. Gurung M, Adhikari BB, Khunathai K, Kawakita H, Ohto K, Harada H, et al. Quaternary amine modified persimmon tannin gel: An efficient adsorbent for the recovery of precious metals from hydrochloric acid media. *Sep Sci Technol*. 2011;46(14):2250–9. <https://doi.org/10.1080/01496395.2011.594698>
21. Calzaferri G, Gallagher SH, Brühwiler D. Multiple equilibria describe the complete adsorption isotherms of nonporous, microporous, and mesoporous adsorbents. *Microporous Mesoporous Mater*. 2022;330:111563. <https://doi.org/10.1016/j.micromeso.2021.111563>
22. Salim NAA, Puteh MH, Yusoff ARM, Abdullah NH, Fulazzaky MA, Rudie Arman MAZ, et al. Adsorption isotherms and kinetics of phosphate on waste mussel shell. *Malaysian J Fundam Applied Sci*. 2020;16(3):393–9. <https://doi.org/10.11113/mjfas.v16n3.1752>
23. Dada AO, Olalekan AP, Olatunya AM, Dada O. Langmuir, Freundlich, Temkin and Dubinin–Radushkevich isotherms studies of equilibrium sorption of Zn²⁺ onto phosphoric acid modified rice husk. *IOSR J Appl Chem*. 2012;3(1):38–45. <https://doi.org/10.9790/5736-0313845>
24. García-Calzón JA, Díaz-García ME. Characterization of binding sites in molecularly imprinted polymers. *Sensors Actuators B Chem*. 2007;123(2):1180–94. <https://doi.org/10.1016/j.snb.2006.10.068>
25. Nakhjiri MT, Bagheri Marandi G, Kurdtabar M. Adsorption of methylene blue, brilliant green and rhodamine B from aqueous solution using collagen-gp (AA-co-NVP)/Fe₃O₄@ SiO₂ nanocomposite hydrogel. *J Polym Environ*. 2019;27:581–99. <https://doi.org/10.1007/s10924-019-01372-8>
26. Samadi N, Hasanzadeh R, Rasad M. Adsorption isotherms, kinetic, and desorption studies on removal of toxic metal ions from aqueous solutions by a polymeric adsorbent. *J Appl Polym Sci*. 2015;132(11). <https://doi.org/10.1002/app.41642>
27. Togue Kanga F. Modeling adsorption mechanism of paraquat onto Ayous (*Triplochiton scleroxylon*) wood sawdust. *Appl Water Sci*. 2019;9(1):1. <https://doi.org/10.1007/s13201-018-0879-3>
28. Singh J, Mishra V. Modeling of adsorption flux in nickel-contaminated synthetic, simulated wastewater in the batch reactor. *J Environ Sci Heal Part A [Internet]*. 2020 Jul 28;55(9):1059–69. <https://doi.org/10.1080/10934529.2020.1767983>.
29. Yu J, Chi R, Zhang Y, Xu Z, Xiao C, Guo J. A situ co-precipitation method to prepare magnetic PMDA-modified sugarcane bagasse and its application for competitive adsorption of methylene blue and basic magenta. *Bioresour Technol*. 2012;110:160–6. <https://doi.org/10.1016/j.biortech.2012.01.134>.
30. Zhang S, Shao T, Kose HS, Karanfil T. Adsorption kinetics of aromatic compounds on carbon nanotubes and activated carbons. *Environ Toxicol Chem*. 2012;31(1):79–85. <https://doi.org/10.1002/etc.724>.
31. Akpomie KG, Dawodu FA, Adebowale KO. Mechanism on the sorption of heavy metals from binary-solution by a low-cost montmorillonite and its desorption potential. *Alexandria Eng J*. 2015;54(3):757–67. <https://doi.org/10.1016/j.aej.2015.03.025>.